Polymer 206 (2020) 122871

Contents lists available at ScienceDirect

Polymer

journal homepage: http://www.elsevier.com/locate/polymer

Effect of temperature on the association behavior in aqueous mixtures of an oppositely charged amphiphilic block copolymer and bile salt

Guanqun Du [a], Alessandra Del Giudice [b], Viveka Alfredsson [a], Anna M. Carnerup [a], Nicolae V. Pavel [b], Watson Loh [c], Giancarlo Masci [b], Bo Nyström [d], Luciano Galantini [b,**], Karin Schillén [a,*]

[a] Division of Physical Chemistry, Department of Chemistry, Lund University, P.O. Box 124, SE-221 00, Lund, Sweden
[b] Department of Chemistry, Sapienza University of Rome, P.le A. Moro 5, I-00185, Roma, Italy
[c] Institute of Chemistry, University of Campinas (UNICAMP), P.O. Box 6154, 13083-970, Campinas, SP, Brazil
[d] Department of Chemistry, University of Oslo, P.O. Box 1033, Blindern, N-0315, Oslo, Norway

ARTICLE INFO

Keywords:
Oppositely charged polymer-surfactant systems
Bile salts
Cationic thermoresponsive block copolymers

ABSTRACT

The association in aqueous mixtures of a thermoresponsive cationic diblock copolymer composed of poly(*N*-isopropylacrylamide) (PNIPAM) and poly(3-acrylamidopropyl)-trimethylammonium-chloride (PAMPTMA(+)) and the oppositely charged bile salt sodium deoxycholate (NaDC) is investigated at different compositions by light and X-ray scattering, calorimetry, and electrophoretic mobility measurements. Clouding reveals aggregation upon heating. The addition of NaDC to the copolymer solution lowers the temperature of the transition and increases its cooperativity. At high temperature and low NaDC fractions, mixed aggregates with a dehydrated PNIPAM-rich interior and a PAMPTMA(+)-rich shell partially neutralized by DC^- anions are formed. At high NaDC fractions, the aggregates present internal regularly spaced segregated nanoregions of dehydrated PNIPAM and PAMPTMA(+)/DC^- (microphase separation). The results suggest that the mixed aggregates have appealing composition-controlled thermoresponse. The system phase separates at body temperature and the highest NaDC fractions investigated, meaning in conditions accomplished when the use of the polymer as a bile salt sequestrant is hypothesized.

1. Introduction

The need to develop new stimuli-responsive self-assembling bio-colloidal systems, which are responding to temperature and/or other types of external stimuli, has increased with the fast growth in the field of nanomaterials, as well as in medical applications. Co-assembled structures, based on a mixture of thermo-responsive block copolymers and surfactants, can provide other types of smart nanocarriers for inclusion, transport, and delivery of biomolecules or active drug substances. Especially biocompatible thermoresponsive polymers and surfactants are particularly interesting [1–4].

Bile salts (BSs) are anionic biological surfactants with a rigid steroidal amphiphilic structure completely different from the typical head-tail one of conventional surfactants. As end-products of the cholesterol metabolism, BSs (often termed bile acids (BAs) referring to their protonated forms) help the small intestine to solubilize dietary lipids and absorb fat-soluble vitamins from foods and are thus extremely important for most living organisms [5–7]. Many bile-acid related diseases, such as BA diarrhea (BAD) caused by BAs in the large intestine or colon, are related to the malabsorption of BSs in the small intestine (secondary BAD) or to a defective fibroblast growth factor 19 (FGF19) feedback inhibition of the biosynthesis of BAs in the liver that in turn leads to a BA overproduction (primary BAD) [8–11]. In the medical treatment of those diseases, oppositely charged polyelectrolytes are used as BS (often BA) sequestrants to bind the BSs through both electrostatic and hydrophobic attractive interactions to hinder them from contact with the colonic mucosa and as such decrease the BS level in the colon [5,12–15]. BS sequestrants are also important drugs used in the treatment of hypercholesterolemia where lowering the level of cholesterol in the body is necessary. The currently used sequestrants bind un-specifically to BS in

* Corresponding author.
** Corresponding author.
E-mail addresses: Luciano.Galantini@uniroma1.it (L. Galantini), Karin.Schillen@fkem1.lu.se (K. Schillén).

https://doi.org/10.1016/j.polymer.2020.122871
Received 17 May 2020; Received in revised form 26 July 2020; Accepted 29 July 2020
Available online 5 August 2020

the small intestine interrupting the enterohepatic circulation to the liver, where the increased conversion of cholesterol leads to the lowering of the LDL (low-density lipoproteins, "bad") cholesterol in the blood, and simultaneously to an unavoidable increase in the HDL (high-density lipoproteins, "good") cholesterol and triglycerides, see Ref. [16,17] and the references therein. BS sequestrants can also reduce glucose levels in patients with type 2 diabetes mellitus, although the mechanism of action still remains unclear [18].

There is yet room for improvement of the currently used sequestrants of water-insoluble cationic hydrogels that have poor patient compliance [13,15] and recently some reports on new polymeric BS sequestrants have appeared in the literature [19,20]. BS sequestrants based on new water-soluble biocompatible substances such as block copolymers that interact strongly both electrostatically and hydrophobically could be considered as compelling alternatives [21–23]. We have in earlier studies investigated the interaction between BSs and triblock copolymers composed of a hydrophobic middle block of poly(propylene oxide) (PPO) and two hydrophilic end-blocks of poly(ethylene oxide) (PEO) [24–26]. References to other groups' studies on PEO-PPO-PEO/BS systems can be found in the work by Patel et al. [27]. PEO-PPO-PEO copolymers are thermoresponsive block copolymers that self-assemble into micelles with a PPO core upon an increase in temperature [28–31] and their use in medical formulations is highly relevant [32,33]. Overall, our studies on block copolymer/BS systems aim to elucidate the co-assembly behavior in the mixed systems, and by that give indication on how and which types of block copolymers may be used for the aforementioned medical applications. Because the BSs are anionic surfactants, it is expected cationic block copolymers would in general provide better performance for the BS binding applications discussed here.

With this in mind, we turned our attention to cationic diblock copolymers consisting of one block of poly(*N*-isopropylacrylamide) PNIPAM and one cationic block of poly(3-acrylamidopropyl)-trimethylammonium chloride (PAMPTMA(+)) (denoted PNIPAM$_m$-*b*-PAMPTMA(+)$_n$, where *m* and *n* are the degrees of polymerization). Like many of the PEO-PPO-PEO copolymers, these polymers are biocompatible and due to the PNIPAM block, they have a thermoresponsiveness suitable for biotechnological applications [34]. PNIPAM-based block copolymers with one or several charged or nonionic hydrophilic blocks self-assemble in water into micelles or other types of structural aggregates with increasing temperature, in which the hydrophilic polymer chains protect a hydrophobic interior composed of the PNIPAM blocks. The micelle formation and phase behavior of PNIPAM-based block copolymers have been extensively reported in the literature, see, e.g., Refs. [35–52] and the references therein. The self-association is a direct effect of the change in aqueous solubility of PNIPAM with increasing temperature. Aqueous systems of thermoresponsive homopolymers, such as PNIPAM, demix at temperatures above the lower critical solution temperature (LCST) of the polymer as a result of its loss of water solubility due to a decrease of polymer-water hydrogen bonds, and at the same time due to the increase of intramolecular hydrogen bonds and hydrophobic interactions [53–62]. LCST of PNIPAM is usually quoted as 31 °C or 32 °C [63,64], whereas the demixing or cloud point temperature (T_{cp}) varies in the range 24–44 °C depending on molecular weight, polydispersity, concentration and method of characterization [60,64–66]. The aqueous phase behavior of PNIPAM is discussed in detail in a recent review by Halperin et al. [64].

In order to investigate the potential of using PNIPAM$_m$-*b*-PAMPTMA(+)$_n$ copolymers as BS sequestrants, we have performed studies on the interaction and complex formation between a specific copolymer (PNIPAM$_{120}$-*b*-PAMPTMA(+)$_{30}$) and a natural [23] or a synthetically modified [67] bile salt. In these studies, we demonstrated that intriguing supramolecular structures are formed when mixing the two oppositely charged species involving both attractive electrostatic and hydrophobic intermolecular interactions. Besides their potential in BS sequestration, mixed complexes of biocompatible copolymers and BSs have recently drawn significant interest, such as in formulations of drug carriers based on electrostatically assisted assembly [68–70]. The unconventional amphiphilic features of BSs, which sometimes are emphasized in synthetically modified derivatives, further motivated the interest of these complexes [71,72]. However, the temperature effects on the behavior of these copolymer–BS mixed complexes especially for medical applications should also be underlined and deeply understood.

In this work, we have extended our previous study on the PNIPAM$_{120}$-*b*-PAMPTMA(+)$_{30}$/NaDC system [23], which focused on the interactions and co-assembled structures in the system at 25 °C, to also explore the effect of temperature on the association behavior of the system. The temperature studied here was in a broad range covering body temperature and reaching elevated temperatures above the cloud point of PNIPAM. Samples at BS/copolymer charge ratios below and above the value at charge equimolarity were investigated to comprehensively highlight the effect of composition on the thermoresponse. A combination of light and X-ray scattering techniques, electrophoretic mobility, and differential scanning calorimetry (DSC) measurements were used to gain insight into the temperature-dependent assembly in the PNIPAM$_{120}$-*b*-PAMPTMA(+)$_{30}$/NaDC system.

2. Methods and materials

2.1. Materials

The diblock copolymer PNIPAM$_{m=120}$-*b*-PAMPTMA(+)$_{n=30}$ with a nominal molar mass $M = 19\,871$ g mol^{-1} (*m* and *n* were determined from proton nuclear magnetic resonance, NMR) and number-average molar mass M_n = 20 000 g mol^{-1} (from gel permeation chromatography (GPC), polydispersity was M_w/M_n = 1.20, where M_w is the weight-average molar mass) was synthesized by atom transfer radical polymerization (ATRP), which is described in Refs. [23,38]. The homopolymer PNIPAM$_{97}$ ($M = 11\,077$ g mol^{-1}, $M_n = 12\,300$ g mol^{-1} and M_w/M_n = 1.17) was synthesized by ATRP as described in Ref. [73]. The bile salt sodium deoxycholate (NaDC) with M = 414.55 g mol^{-1} was purchased from Sigma Aldrich (assay ≥ 99%) and used as received. Fig. 1 illustrates the molecular structures of the two chemical species.

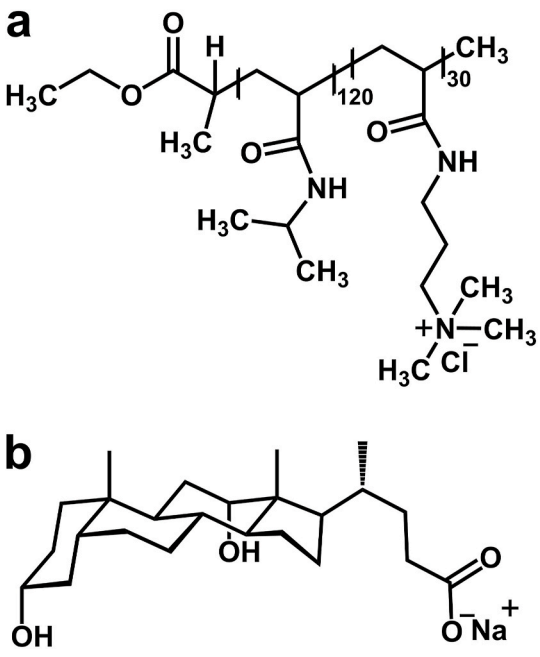

Fig. 1. Molecular structures of (a) the diblock copolymer PNIPAM$_{120}$-*b*-PAMPTMA(+)$_{30}$ and (b) NaDC studied in this work.

2.2. Sample preparation

All solutions of PNIPAM$_{120}$-*b*-PAMPTMA(+)$_{30}$ copolymer and NaDC were prepared with water purified using a Milli-Q system (Millipore Corporation, Bedford, MA). The sample preparation is described in detail in Ref. [23]. The composition is expressed in molar fraction of negative charge, defined as $X = n_-/(n_- + n_+)$, where n_- and n_+ are the number of moles of negative charges (= number of moles of NaDC) and number of moles of positive charges (= 30 × number of moles of PNIPAM$_{120}$-*b*-PAMPTMA(+)$_{30}$), respectively. The PNIPAM$_{120}$-*b*-PAMPTMA(+)$_{30}$–NaDC mixed solutions were prepared with a constant copolymer concentration of 0.13 wt% and varying NaDC content (0.49, 0.98, 1.96, 3.93, 7.85, 15.7, 31.4 mM) so that X is equal to 0.20, 0.33, 0.50, 0.67, 0.80, 0.89 and 0.94, respectively. These charge fractions correspond to bile salt-to-copolymer molar charge ratios (CR = n_-/n_+) between 0.25 and 16 (X or CR = 0 denotes the pure block copolymer). *M* values from NMR were used in all concentration calculations. The mixed solutions used in the light scattering and electrophoretic mobility experiments were filtered through 0.45 μm-Millex-HV syringe filters from Millipore (now Merck Millipore) prior to the measurements. In the case of the DSC and small angle X-ray scattering (SAXS) experiments, the solutions studied were not filtered and they had a higher fixed copolymer concentration (0.50 wt%) to produce a good signal.

2.3. Dynamic light scattering

A Zetasizer Nano ZS instrument from Malvern Instruments, Ltd., Worcestershire, U.K was utilized to perform temperature dependent dynamic light scattering (DLS) measurements in a backscattering geometry at a scattering angle of $\theta = 173°$ using DTS1070 disposable folded capillary cells [74]. The instrument is equipped with a He−Ne laser ($\lambda = 632.8$ nm, 4 mW) with an automatic laser attenuator, and the detection unit comprises an avalanche photodiode. The temperature interval ranged from 20 to 60 °C. Increments of 2 °C were used and with a delay time of 120 s after each increment to ensure equilibrium of the system.

The obtained time autocorrelation functions of the scattered intensity were evaluated by the Cumulant method [75,76]. In this analysis, the logarithm of the normalized electric field autocorrelation function $g^{(1)}(t)$, obtained from the normalized intensity autocorrelation function $g^{(2)}(t)$ through $g^{(2)}(t) - 1 = \beta\left|g^{(1)}(t)\right|^2$, is expressed as a Taylor expansion to which the experimental data is fitted:

$$\ln\left(\sqrt{g^{(2)}(t) - 1}\right) = \frac{1}{2}\ln\beta - \langle\Gamma\rangle t + \frac{1}{2}\mu_2^2 t^2 \ldots \quad (1)$$

where the first cumulant is the same as the average of the relaxation rate $\langle\Gamma\rangle$ and μ_2 is the second cumulant. β is the coherence factor taking into account deviations from ideal correlation and experimental geometry (in this work, β was typically 0.9).

The result of the Cumulant analysis is presented in this work as a mean relaxation time $\langle\tau\rangle$ (here defined as $\langle\tau\rangle = 1/\langle\Gamma\rangle$, see Eq (1)) or, to account for changes in the absolute temperature and solvent viscosity, the reduced mean relaxation time $\langle\tau\rangle T/\eta_0$. Using $\langle\tau\rangle$ allowed for conveniently follow the effect of NaDC on the temperature-dependent solution behavior at a finite concentration. Both the DLS data and the simultanously recorded total light scattering intensity (I_{tot}) (without any subtraction of the solvent scattering) are presented as the average of three consecutive measurements together with the estimated standard deviation (*std*) at each temperature.

2.4. Electrophoretic mobility measurements

Measurements of the electrophoretic mobility (μ) at different temperatures were performed at $\theta = 13°$ using the same instrumental setup and type of cuvettes as for the light scattering experiments, see Ref. [23] for more details. The μ values are presented as the average of three consecutive measurements together with the estimated *std*. They were not corrected for the change in solvent viscosity with temperature.

2.5. High-sensitivity differential scanning calorimetry

A MicroCal VP-high-sensitivity differential scanning calorimeter from Malvern Instruments (now Malvern Panalytical Ltd), Malvern, United Kingdom was used to perform the DSC measurements on the mixed solutions. The instruments have two cells of 0.5065 mL, one for the sample and one for the solvent reference (here water). For all samples, two to three consecutives up and down scans in temperature were carried out in the range 5–80 °C with a scanning rate of 0.5 °C min^{-1}. The sample was injected cold into the sample cell at 5 °C and was let to equilibrate for 15 min before the first up scan was started. The down scan started immediately after reaching the highest temperature and once reached 5 °C, the sample was allowed to equilibrate for 5 h before the second up scan was performed. In some cases, a third set of scans was executed. Identical up scans were obtained, which demonstrates that the solutions may return to the homogenous one-phase after storage at low temperature. The thermograms are expressed as apparent molar heat capacity ($C_{p,app}$) versus temperature.

2.6. Small angle X-ray scattering

SAXS measurements were performed at the SWING beamline of SOLEIL Synchrotron Facility (Saint-Aubin, France) with the beam energy of 12.0 keV. Scattering data were collected using a 17 × 17 cm^2 low-noise AVIEX CCD detector with q values ranging in the interval from 0.023 nm^{-1} to 3.4 nm^{-1} ($q = \frac{4\pi}{\lambda}\sin(\theta/2)$ and θ is the scattering angle). An automated robot provided at the beamline was used in the experiments [77]. In order to avoid possible beam damage of the samples, the measurements were performed using a continuous flow of the investigated solution (50 μL min^{-1}) in front of the beam. The capillary and the solution were equilibrated at each investigated temperature before sample injection. The SAXS data reduction (radial averaging, background subtraction, absolute intensity calibration with water [78]) was performed using the FoxTrot software (https://www.synchrotron-soleil.fr/en/beamlines/swing) developed at the beamline.

3. Results and discussion

We have previously demonstrated using cryo-transmission electron microscopy (cryo-TEM) that the PNIPAM$_{120}$-*b*-PAMPTMA(+)$_{30}$ block copolymer and NaDC form mixed complexes with intriguing morphologies at 25 °C [23]. In order to complement our previous study, we here report on the thermoresponsive behavior of the PNIPAM$_{120}$-*b*-PAMPTMA(+)$_{30}$–NaDC mixtures to retrieve information about temperature-induced interactions and association of the systems at elevated temperatures. The dilute mixed solutions were investigated at compositions below and above charge neutralization in the range $0 \leq X \leq 0.94$ and in the temperature range 5–80 °C.

3.1. Light scattering measurements

The thermoresponsive behavior of the pure copolymer solution and the mixed solutions of the copolymer and BS was explored by analyzing the total scattered intensity as a function of temperature. The data are presented in Fig. 2.

We have previously demonstrated that mixed supramolecular tape-like structures are formed in aqueous mixtures of PNIPAM$_{120}$-*b*-PAMPTMA(+)$_{30}$ and NaDC at 25 °C as a result of the electrostatic interaction between the DC$^-$ anions and the PAMPTMA(+) blocks of the copolymers and hydrophobic bile salt-bile salt interactions [23]. This

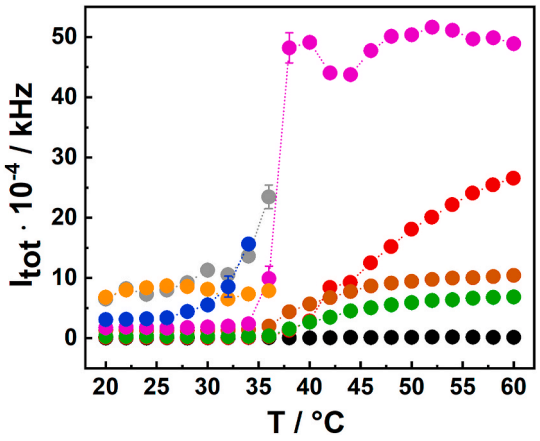

Fig. 2. The total light scattering intensity (I_{tot}) (without any subtraction of the solvent scattering) as a function of temperature of aqueous solutions of PNIPAM$_{120}$-*b*-PAMPTMA(+)$_{30}$ and NaDC at different charge fractions (X): X = 0 (black, pure copolymer solution), X = 0.20 (red), X = 0.33 (brown) X = 0.50 (green), X = 0.67 (blue), X = 0.80 (magenta), X = 0.89 (orange) and X = 0.94 (grey). The samples with X = 0.67, 0.89 and 0.94 were not investigated in the precipitation region occurring at elevated temperatures. The copolymer concentration was 0.13 wt% in the mixtures. The concentration of the pure copolymer solution was 0.20 wt%. The error bars (± *std* of three consecutive measurements) are within the size of the symbols. The interpolating lines are guides to the eye. (For interpretation of the references to color in this figure legend, the reader is referred to the Web version of this article.)

strong intermolecular interaction is also reflected by the fact that the temperature response of the mixed solutions altered significantly in comparison to the pure copolymer solution, for which I_{tot} was very low over the whole temperature range. As observed in Fig. 2, the scattering intensity of the mixed solutions increased sharply at a specific transition temperature. The cloud point temperatures were determined from the initial rise in I_{tot}. Except for X = 0.67, 0.89 and 0.94 that precipitated above 34/36 °C (Fig. S2), the T_{cp} values are in the range of 34–36 °C. Slightly higher values (36–40 °C) were determined from the inflection point of the curves as estimated from its first derivative (Fig. S1). The presented light scattering results illustrate that the thermoresponsive performance of the PNIPAM$_{120}$-*b*-PAMPTMA(+)$_{30}$/NaDC system leads to pronounced association into large copolymer-bile salt aggregates (or precipitation) reflecting the change in water-solubility of PNIPAM at elevated temperatures.

In line with our results, precipitation has been reported [79,80] to take place for mixtures at elevated temperatures in oppositely charged PNIPAM copolymer-surfactant systems as the PNIPAM parts dehydrate and remove the steric repulsion between the particles. The precipitation at X = 0.67 (i.e., charge ratio, CR = 2), can be explained by that this sample contained complexes with an electrophoretic mobility close to zero at 25 °C (see Ref. [23]). This observation is further discussed in connection with the results from the electrophoretic mobility experiments. The precipitation occurring in the mixed solutions with the highest charge fractions of bile salt (X ≥ 0.89, CR ≥ 8) is probably caused by the significant ionic strength due to the high bile salt concentration. As these BS concentrations are higher than CMC, depletion effects from NaDC micelles could also contribute to the precipitation of the aggregates.

DLS measurements were carried out on the filtered block copolymer–BS mixed solutions and pure copolymer solution as a function of temperature. It should be noted that whereas the unfiltered mixed solutions contain co-existing globular and tape-like complexes, the latter is the dominant structure after filtration [23]. Fig. 3a displays the time autocorrelation functions of the scattered intensity for a mixed sample with equimolar charge composition (i.e., X = 0.50) measured at various temperatures between 20 and 60 °C. They demonstrate a noticeable shift toward longer times at around 36 °C, indicating aggregate growth, thus corroborating the increase in scattering intensity seen in Fig. 2. The corresponding relaxation time distributions obtained from inverse Laplace transformation by non-linear least square (NNLS) analysis are presented in the inset of Fig. 3a.

The tape-like copolymer-bile salt mixed complexes of several micrometer in length as detected by cryo-TEM at 25 °C [23] do not allow for an unambiguous interpretation of the relaxation time distributions at X = 0.50. In Ref. [23], the distributions obtained from regularized inverse Laplace transformation (REPES) analysis of the pseudo-cross correlation

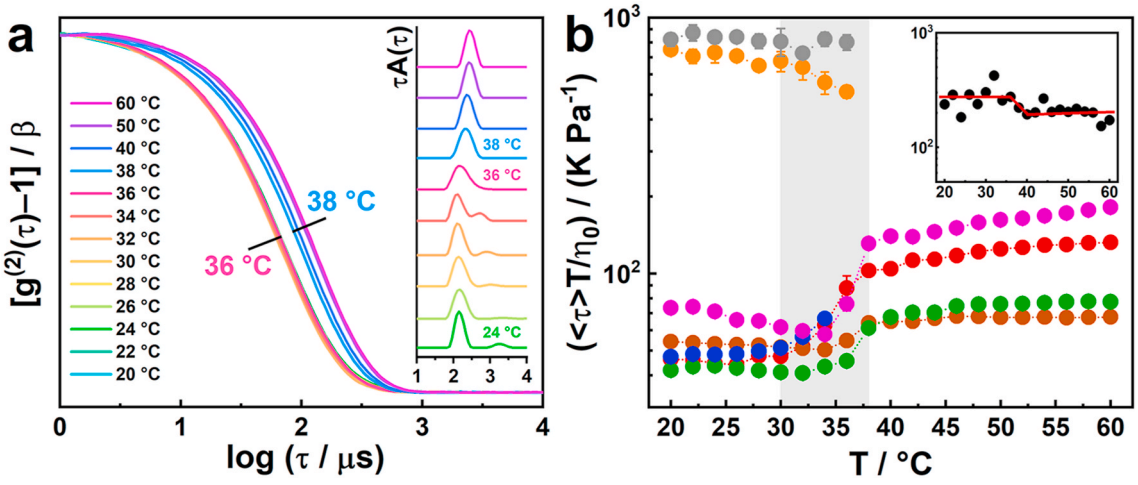

Fig. 3. (a) Normalized autocorrelation functions of the scattered intensity for the PNIPAM$_{120}$-*b*-PAMPTMA(+)$_{30}$–NaDC mixed solution at X = 0.50 (CR = 1) and the corresponding relaxation time distributions obtained from NNLS analysis (inset) at the different temperatures indicated. The x-axis is corrected for the change in absolute temperature and solvent viscosity relative to 20 °C by multiplying a correction factor of $(T/\eta_0)/(293/\eta_{293})$; (b) The temperature dependence of the reduced mean relaxation time from Cumulant analysis ($\langle\tau\rangle T/\eta_0$) of aqueous solutions of PNIPAM$_{120}$-*b*-PAMPTMA(+)$_{30}$ and NaDC at different charge fractions (X): X = 0 (inset, black), X = 0.20 (red), X = 0.33 (brown), X = 0.50 (green), X = 0.67 (blue), X = 0.80 (magenta), X = 0.89 (orange) and X = 0.94 (grey). The transition regime is marked light grey. The samples with X = 0.67, 0.89 and 0.94 were not investigated above the precipitation region occurring at elevated temperatures. The copolymer concentration was 0.13 wt% in the mixtures. The concentration of the pure copolymer solution was 0.20 wt%. The error bars are ± *std* of three consecutive measurements. The interpolating lines are guides to the eye. (For interpretation of the references to color in this figure legend, the reader is referred to the Web version of this article.)

functions at different angles clearly exhibited two relaxation modes (see Supporting information of ref [23]). A slow mode, which was attributed to translational diffusion ($\tau_{slow} \propto q^{-2}$) possibly connected to the shorter tapes in the population that were within the size range of detection ($qR_g < 1$), and a fast relaxation mode, which was proposed to be related to a translational diffusion-coupled internal motion mode linked to the some kind of thermal bending fluctuations of the tape. The relative amplitude of the fast mode was observed to increase on the expense of that of the slow mode with increasing scattering angle up to $\theta = 145°$, which was the maximum angle of that study. In accordance with the data of ref [23], we notice that the bimodal feature of the relaxation time distributions at temperatures below T_{cp} (36 °C) is still present in Fig. 3a, however the modes are less resolved in comparison. Furthermore, as observed in the figure, the relative amplitude of the slow mode is small, as compared to the fast mode, with a significant uncertainty of position. It is also much less dominant than what was observed at $\theta = 145°$ [23]. In our present study, DLS measurements were performed at fixed angle of 173°, which could explain these differences in peak amplitude and the diminishing slow mode compared to our previous work. At such high angle, the scattering is further reduced because of the strong angular dependence of the form factor of large extended structures (high destructive interference), which leads to $qR_g \gg 1$ and a smaller portion of the population is monitored. At temperatures above T_{cp}, reasonably monomodal distributions corresponding to the translational diffusion of aggregates are found.

Because of these complicated relaxation processes below the transition temperatures, the mean relaxation time obtained from the Cumulant analysis was considered to follow the temperature-dependent association behavior of the PNIPAM$_{120}$-*b*-PAMPTMA(+)$_{30}$/NaDC system as a function of composition (Fig. 3b). For the pure block copolymer solution (X = 0), very noisy autocorrelation functions were measured due to the low scattered intensity and poor statistics. As established earlier [36,42,43,46,51,80], at temperatures below the phase transition temperature of PNIPAM, PNIPAM-based block copolymers can be present as single polymer coils (unimers) in dilute aqueous solution co-existing with a few large multi-chain aggregates ("clusters") due to the fact that PNIPAM is an amphiphilic polymer [59]. In the inset of Fig. 3b, a step-wise lowering of the reduced mean relaxation time is shown at 36–40 °C, suggesting a shrinkage of these clusters with temperature, which implies a decrease roughly from 280 to 200 nm in apparent mean hydrodynamic diameter $\langle D_H \rangle$ as calculated from Stokes-Einstein relation. This behavior can also be easily observed in the hydrodynamic diameter distributions from NNLS analysis as shown in Fig. S3. As noticed, bimodal distributions dominated by the slow cluster mode are obtained at low temperatures, while above the transition temperature regime, the distributions become monomodal and shift towards smaller sizes as more compact aggregates are formed, in coherence with the study of Bayati et al. [43].

In the case of the PNIPAM$_{120}$-*b*-PAMPTMA(+)$_{30}$–NaDC mixed solutions, the DLS data allow us to identify two types of thermal behaviors (Fig. 3b). The relaxation time versus temperature shows a significant increase within a transition regime (30–36 °C) and levels off at higher temperatures for both the mixtures with a low fraction of bile salt (X = 0.20, 0.33, 0.50 or CR = 0.25, 0.50, 1) and for the samples with exceeding bile salt charge fraction with the exception of the samples at X = 0.67, 0.89 and 0.94, where precipitation took place (data also reported in Fig. S2). We find that $\langle D_H \rangle$ of the aggregates at 60 °C is equal to 135.2 nm, 69.0 nm, 79.5 nm and 186.0 nm at X = 0.20, 0.33, 0.50 and 0.80, respectively, thereby showing that a lowering of the aggregate size occurs at the first additions of the BS, whereas a growth takes place beyond a certain threshold of BS fraction (X = 0.33). In addition, interestingly, an initial fastening of the relaxation times of the X = 0.80 was observed, which indicates a shrinkage of the assembling complexes prior to the transition (Fig. 3b).

The samples with the highest charge fractions (X = 0.89 and 0.94) showed a less regular temperature behavior (Fig. S2b). The reduced mean relaxation times ($\langle \tau \rangle T/\eta_0$) at low temperature were significantly slower than those obtained for solutions with lower NaDC fraction (Fig. 3b). Like the I_{tot} data (Fig. 2), the values are constant up to about 36 °C. Above this temperature, the aggregation process induced precipitation.

3.2. Electrophoretic mobility measurements

The effect of temperature on the association behavior of the PNIPAM$_{120}$-*b*-PAMPTMA(+)$_{30}$/NaDC mixtures was revealed by changes in the mean electrophoretic mobility, which was measured at different compositions (0 ≤ X ≤ 0.94) as a function of temperature.

Starting from electrophoretic mobility values close to zero at ambient temperatures, it is observed that for mixtures with X = 0.50 and below, μ increased steeply with increasing temperature at a certain critical temperature (typically around 34 °C) to reach a maximum plateau value (between $4.5{\cdot}10^{-8}$ – $7.2{\cdot}10^{-8}$ $m^2s^{-1}V^{-1}$). This temperature coincides with T_{cp} obtained from the total scattering intensity in each case. Interestingly, these data implies that at X = 0.50 (CR = 1), for which the electrophoretic mobility is positive (at all temperatures), a fraction of bile salt not participating in the complex was present at charge equimolar composition, as verified in similar block copolymer-surfactant mixtures reported in literature [81,82].

The DLS results presented in chapter 3.1 indicate that in the case of the pure block copolymer solution, the dehydration of the PNIPAM blocks induces shrinkage of the copolymer clusters (Fig. 3b, inset). In addition, we believe that the dehydration makes some of the free unimers, which coexist with the clusters at low temperature, associate with the copolymer-BS mixed aggregates above the transition temperature. The two effects result in the formation of aggregates at high temperature with less hydration water and thereby a higher charge density (charge/volume ratio), which in turn is reflected in an increase of the electrophoretic mobility with temperature as shown in Fig. 4 for the pure block copolymer. This result is in agreement with what has been reported before for pure copolymers of the same kind [43].

In the mixtures, the complexes formed by co-assembly at low temperatures [23] rearrange into copolymer-BS aggregates of different structures above the transition temperature. Typical aggregates can be

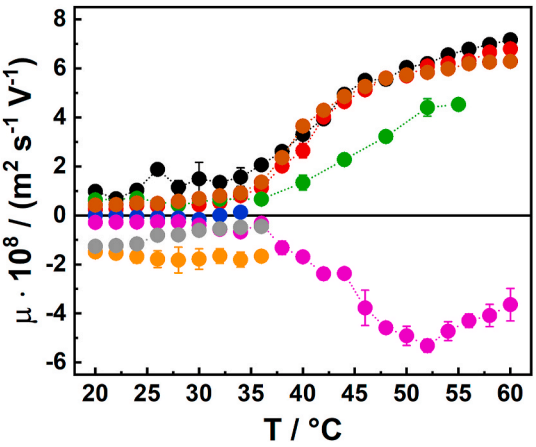

Fig. 4. The temperature dependence of the average electrophoretic mobility (μ) of aqueous mixtures of PNIPAM$_{120}$-*b*-PAMPTMA(+)$_{30}$ and NaDC at different charge fractions (X): X = 0 (black, pure copolymer solution), X = 0.20 (red), X = 0.33 (brown), X = 0.50 (green), X = 0.67 (blue), X = 0.80 (magenta), X = 0.89 (orange) and X = 0.94 (grey). The samples with X = 0.67, 0.89 and 0.94 were not investigated in the precipitation region occurring at elevated temperatures. The copolymer concentration was fixed at 0.13 wt%. The error bars (± *std* of three consecutive measurements) are within the size of the symbols. The interpolating lines are guides to the eye. (For interpretation of the references to color in this figure legend, the reader is referred to the Web version of this article.)

envisioned either having a core-corona architecture with an interior containing dehydrated PNIPAM and DC^- neutralized PAMPTMA(+) segments or formed by partially BS neutralized copolymer chains with less dehydrated PNIPAM blocks (see DSC and SAXS results and discussion in chapters 3.3 and 3.4). Whatever the structure of the aggregates, like for the pure copolymer system, reaching the transition temperature, PNIPAM dehydration (i.e., compaction) occurs, which leads to an increase of the charge density of the aggregates. This effect, together with specific effects related to the structural rearrangements, leads to an increase of the μ values. In addition, for the mixtures at low NaDC fraction (X = 0.20 and 0.33, i.e., CR = 0.25 and 0.50), a significant fraction of non-associated block copolymers is expected to be in equilibrium with the mixed complexes, we believe that the loss of the PNIPAM water solubility also promotes an extensive association of those copolymers to the aggregates. Overall, the trends are in line with those found for mixtures of the same copolymer but containing a bile salt derivative instead of NaDC [67].

At a high charge fraction (X = 0.80, CR = 4) an opposite trend of the electrophoretic mobility was recorded with a lowering toward significantly negative values (between $-5.3 \cdot 10^{-8}$ and $-3.6 \cdot 10^{-8}$ $m^2 s^{-1} V^{-1}$). In this mixture, large aggregates form when increasing the temperature, however, there is a large fraction of amphiphilic bile salt molecules not interacting with the block copolymer at low temperature and that could associate to the copolymer-BS mixed aggregates (a charge reversal process) as they become increasingly hydrophobic upon increasing temperature. This association process prevented the aggregates from precipitating due to increased repulsive interaction, even though the PNIPAM blocks were dehydrated.

As reported in our previous paper the μ value for the X = 0.67 sample at room temperature is around zero [23]. This fraction represents the crossover point between complexes having μ values slightly positive at lower X or slightly negative at higher X. It therefore experienced the highest tendency of precipitation when increasing the temperature. For this sample, the hydrophobic interaction determined an enhanced growth of the aggregates that finally precipitated out of the solution as confirmed by visual inspection. The sedimentation of the precipitates led to significant decrease in scattering intensity above 34 °C and no further measurements were performed in the precipitation regime. As mentioned before, precipitation also occurred at the highest X values investigated (X ≥ 0.89) as a result of that the concentration of NaDC is high and well above CMC.

3.3. DSC measurements

High-sensitivity DSC is a technique well suited to follow thermal transitions in polymer-surfactant solutions, which makes it an interesting method in our case to gain detailed information (direct or indirect) on the interaction between the block copolymer and the bile salt. Because of the entropically favorable release of water (i.e., dehydration) occurring at the phase transition of PNIPAM, DSC has previously been successfully employed to study PNIPAM/water systems, as well as to follow the onset of demixing upon heating [42,83–87]. Other experimental methods have also been employed to investigate the phase transition of PNIPAM, see, e.g., Refs. [64,88] and the references therein. The temperature dependent phase behavior of PNIPAM in water can be tuned by the addition of different kinds of charged surfactants [54,89–91].

To find evidence of our hypothesis that the origin of the temperature-induced association process found in the $PNIPAM_{120}$-*b*-$PAMPTMA(+)_{30}$–NaDC mixed solutions is due to the temperature dependent phase behavior of PNIPAM, we performed DSC measurements on a selection of solutions at X = 0, 0.20, 0.33, 0.50, and 0.80 (CR = 0, 0.25, 0.50, 1.0, and 4.0, respectively). For comparison, pure solutions of the copolymer and a homopolymer with 97 NIPAM units ($PNIPAM_{97}$) were investigated as well. No signal was observed in the DSC thermogram of 100 mM NaDC in water (data not shown) in accordance with the data previously reported for 96 mM sodium glycodeoxycholate in water [24]. The up-scan DSC thermograms are presented in Fig. 5a. We have used the temperature of the onset of the transition peak (T_{onset}) to characterize the phase transitions of the different samples (Fig. 5b). The temperatures of peak maximum (T_{max}) follow the same trend (Fig. 5b and Table 1).

All DSC traces show transition processes with an endothermic transition enthalpy ΔH_{tr} (Table 1). According to previous DSC results on PNIPAM homopolymers [83,92] and the same types of block copolymers [42,87], this process is related to the heat-induced phase transition of PNIPAM. We can thus propose that the signal found in the thermograms of the mixed copolymer-bile salt solutions is related to changes in the water solubility of the PNIPAM block as the light scattering results already anticipated. The pure copolymer data are in good agreement with those reported in Ref. [67] on the same copolymer at a higher concentration (c.f., T_{onset} = 40 °C, ΔH_{tr} = 133 kJ mol^{-1} for 1.0 wt%) (Table 1). T_{onset} and T_{max} are significantly higher than the corresponding temperatures of the $PNIPAM_{97}$ homopolymer solution (Table 1). It is especially worth noting that the transition enthalpy per mole of NIPAM unit measured for $PNIPAM_{97}$ are within the reported range for PNIPAM homopolymers [42,83,89,93]. It should be stressed that the transition temperatures of PNIPAM homopolymers varies with both molecular weight and end-group [66,93]. End effects are increasingly relevant for molecular weights below 15 000 g mol^{-1}. The initiator ethyl 2-chloropropionate used in our case, as well as in Ref. [42], is an uncharged, slightly hydrophobic end group. Both DSC data sets are in agreement to those presented in Ref. [93]. Furthermore, the homopolymer solution presented down-scan traces with a hysteresis towards lower temperatures. Ding et al. have previously reported a hysteresis effect in the DSC traces in the case of PNIPAM samples [85]. This effect could be related to what is reported in Ref. [94], where the authors, by using the temperature-modulated DSC method, suggest that the PNIPAM phase transition can be separated into the endothermic event related to rearrangement of water and a second exothermic event related to the hydrophobic intermolecular interaction between hydrophobic groups in the chain. Moreover, the difference observed between the copolymer and the homopolymer in Fig. 5a has its origin in the electrostatic repulsion between the PAMPTMA(+) blocks of the copolymer unimers. This hinders the aggregation process causing the copolymer to be more soluble at higher temperatures than the homopolymer. For this reason, block copolymer undergoes only a partial dehydration as reflected in the smaller transition enthalpy per mole of NIPAM unit (Table 1), which also are observed for terpolymers of PNIPAM and ionizable acrylic acid groups [95].

A small amount of NaDC present in the $PNIPAM_{120}$-*b*-$PAMPTMA(+)_{30}$ solution altered the picture as represented by the curve at X = 0.20 in Fig. 5a. The shape of the transition changed, as a low-temperature part developed while the remaining high-temperature part was markedly reduced. This caused a significant shift towards lower values of the transition temperatures: $T_{onset} \approx 34$ °C and $T_{max} \approx 36$ °C for X = 0.20 (Table 1). In the solutions at this low bile salt content, there exist some free copolymer chains not involved in the co-assembly into the well-organized copolymer-BS complexes imaged by cryo-TEM at room temperature [23]. We envision a large fraction of these un-complexed copolymers as being assembled into co-existing multi-chain clusters, as revealed in the DLS measurements on the pure copolymer (Fig.3b and Fig. S3). These clusters may also contain some DC^- anions associated by electrostatic interactions. Reaching the phase transition temperature T_{onset}, aggregation occurs due to dehydration of PNIPAM. Since there are un-complexed copolymers present at this point, they aggregate non-cooperatively at a slightly higher temperature, thus justifying the high-temperature "shoulder" of the transition peak. The latter thermal event is better discerned in the inset of Fig. 5a, where the position of the shoulder correlates well with the transition peak of the pure copolymer solution. The thermogram of X = 0.33 also exhibits a "tail" at the high-temperature side of the main peak. Therefore, the DSC data of the mixtures with low NaDC content indicate that there are two PNIPAM

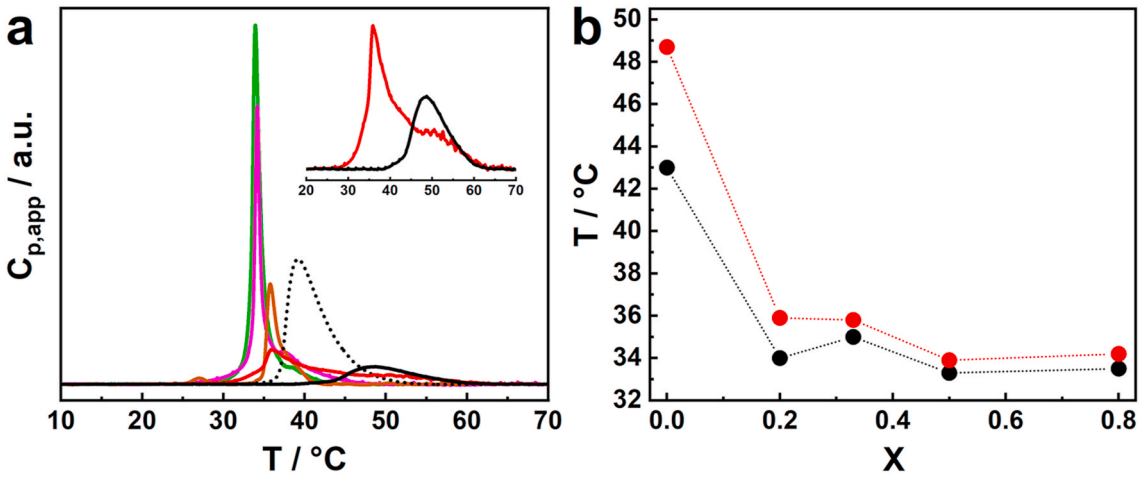

Fig. 5. (a) The apparent heat capacity ($C_{p,app}$) as a function of temperature for aqueous solutions of PNIPAM$_{120}$-*b*-PAMPTMA(+)$_{30}$ and NaDC at different charge fractions (X): X = 0.20 (red), X = 0.33 (brown), X = 0.50 (green), X = 0.80 (magenta) and for pure solutions of copolymer PNIPAM$_{120}$-*b*-PAMPTMA(+)$_{30}$ (X = 0, black solid line) and homopolymer PNIPAM$_{97}$ (black dashed line). The polymer concentration was 0.50 wt% except for X = 0.33 and 0.50, where it was 0.25 wt%. The inset shows the phase transition regime for X = 0 (black) and X = 0.20 (red); (b) The onset temperature T_{onset} (black) and maximum temperature T_{max} (red) of the transition in the DSC traces in (a) as a function of the corresponding charge fraction (X). The interpolating dashed lines are guides to the eye. (For interpretation of the references to color in this figure legend, the reader is referred to the Web version of this article.)

Table 1
Transition enthalpy (ΔH_{tr}), onset (T_{onset}) and maximum (T_{max}) transition temperatures of PNIPAM$_{120}$-*b*-PAMPTMA(+)$_{30}$–NaDC aqueous solutions at different charge fraction (X) and of solutions of pure PNIPAM$_{120}$-*b*-PAMPTMA(+)$_{30}$ and PNIPAM$_{97}$ with polymer concentration ($C_{polymer}$). Scan rate: 30 °C/h.

X[a]	CR[b]	$C_{polymer}$ /mM	ΔH_{tr}[c] /kJ mol^{-1}	T_{onset} /°C	T_{max} /°C
0[d]	0	0.25	132 (1.1)	43.0	48.7
0.20	0.25	0.25	266 (2.2)	34.0	35.9
0.33[e]	0.5	0.12	168 (1.4)	35.0	35.8
0.50[e]	1	0.12	463 (3.9)	33.3	33.9
0.80	4	0.25	396 (3.3)	33.5	34.2
PNIPAM$_{97}$	–	0.45	555 (5.7)	37.0	39.2

[a] $X = n_-/(n_- + n_+)$.
[b] $CR = n_-/(n_+)$.
[c] Value expressed as kJ per mole of PNIPAM (kJ per mole of NIPAM unit in parenthesis).
[d] 0.50 wt% PNIPAM$_{120}$-*b*-PAMPTMA(+)$_{30}$ in water.
[e] Samples with a copolymer concentration of 0.25 wt%.

dehydration events taking place in the mixtures, one cooperative process that could be related to the aggregation of the mixed complexes and one less cooperative aggregation process connected to the BS-containing copolymer clusters. Although it is not possible to obtain structural information from DSC, we could speculate that these different events seem to point towards that at high temperatures, well above the phase transition, the system could include two types of aggregates containing dehydrated PNIPAM. This suggested interpretation is supported by the SAXS analysis presented in chapter 3.4.

The traces of the X = 0.50 and 0.80 mixtures on the other hand display a single, very narrow, transition peak with high amplitude indicative for a highly cooperative process with a $T_{onset} \approx 33$ °C (Fig. 5b) and with corresponding ΔH_{tr} values of 463 and 396 kJ mol^{-1}, respectively (Table 1). The T_{onset} values are in reasonable agreement with the T_{cp} values estimated from SLS measurements. It is clear from comparison of the transition temperatures that the copolymer-BS complex formation at room temperature makes the copolymer less water-soluble, overcompensating the effect of charge of the ionic PAMPTMA(+) block and decreasing the transition temperature down to values lower than that of both the copolymer and the homopolymer (Fig. 5a). In other words, the PNIPAM blocks undergoing this cooperative aggregation process largely belong to the copolymer molecules in which the charged block is engaged in stronger interactions with the bile salt and does not exert the "retarding" shoulder effect on the PNIPAM transition as seen at lower X. Also, the colloidal stability of the system at X = 0.50 and 0.80 above the transition temperature suggests that the inter-aggregate interaction is repulsive and should involve either a positive (X = 0.50) or a negative charge (X = 0.80) of the aggregates at these compositions, see Fig. 4. A perfect overlap of the DSC curve was observed between consecutive scans, demonstrating the reversibility of the thermally induced transition within the 5 h interval between runs (see also long-time experiments reported in Fig. S4).

3.4. SAXS measurements

SAXS measurements were performed on solutions of PNIPAM$_{120}$-*b*-PAMPTMA(+)$_{30}$ and NaDC with X = 0, 0.20, 0.33, 0.50, and 0.80. The temperatures were selected so that the experiments were performed both below and well above their individual transition temperatures (25 and 60 °C, respectively). The SAXS data at 25 °C reported in Ref. [23] showed that the X-ray scattering intensity of the unfiltered sample with X = 0.50 in the measured q range was dominated by the contribution of the globular mixed complexes with extended and soluble PNIPAM corona chains, but the co-existing tape-like complexes were not detectable. The results of the SAXS measurements at 60 °C are presented and compared with the data collected at 25 °C [23] in Fig. 6.

The profile of the pure block copolymer solution shows a growth of the scattered intensity as the temperature increases above the phase transition temperature of PNIPAM (Fig. 6a, right panel). Neglecting the upturn at the lowest q (also seen at 25 °C, Fig. 6a, left panel), which is possibly related to the existence of large clusters [23], the slope of the intensity decay would be compatible to inhomogeneities of the order of 10 nm (Fig. S5). The upturn at low q is preserved at the first addition of NaDC (X = 0.20), meaning that a contribution of large clusters is kept in the SAXS curve. For this sample a general increase of the scattered intensity was observed (Fig. S5), indicating a growth of the average size of the sample inhomogeneities. The very large $\langle D_H \rangle$ values obtained from DLS at X $\leq$ 0.20 confirm the presence of clusters in these samples. With further addition of bile salt, the low q upturn is lost. The indirect Fourier transformation analysis suggests that the scattering curve for the sample with X = 0.33 originates from structures with an average R_g = 17 nm (Fig. S5) and a maximum diameter of 48 nm (Fig. S6a).

At X = 0.50 and 0.80, there is strong increase of the scattered

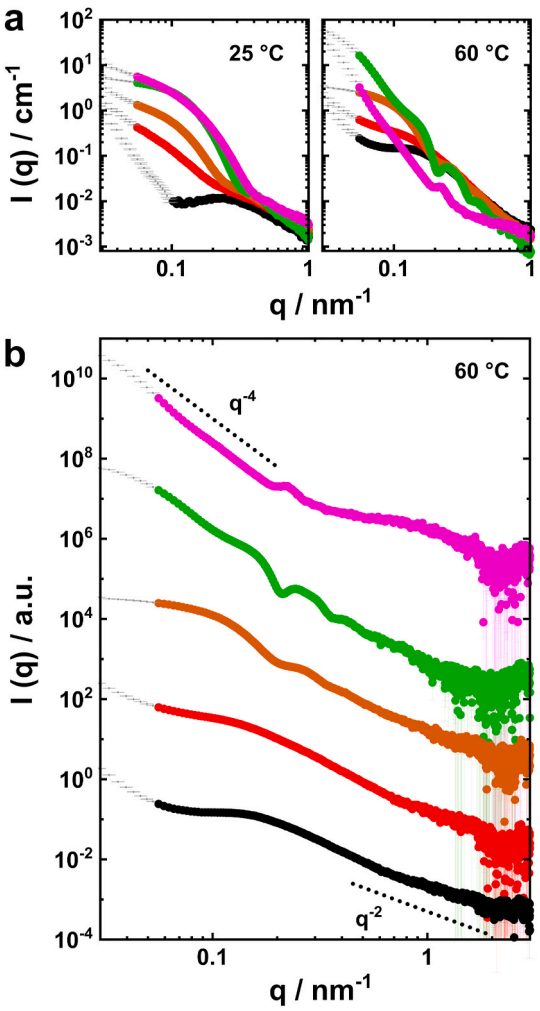

Fig. 6. (a) SAXS curves ($I(q)$ vs. q) on absolute scale at 25 °C (left, adapted from Ref. [23] with permission from the PCCP Owner Societies) and at 60 °C (right) of $PNIPAM_{120}$-*b*-$PAMPTMA(+)_{30}$–NaDC mixed solutions at different charge fractions (X): X = 0 (black, pure copolymer solution), X = 0.20 (red), X = 0.33 (brown), X = 0.50 (green) and X = 0.80 (magenta). The data points not considered for analysis are given in grey. (b) SAXS curves at 60 °C (same as in (a)) with slopes expected for two power-law decay behaviors indicated with dashed lines. The curves have been shifted on the y-axis by a suitable factor to avoid data overlap. The copolymer concentration was 0.5 wt%. (For interpretation of the references to color in this figure legend, the reader is referred to the Web version of this article.)

intensity. This indicates a notable structural rearrangement above the transition temperature with an evident growth of the copolymer–BS aggregates, reaching average dimensions well beyond the Guinier limit. Mainly the tail of the scattering profile of these aggregates is detected at low q, providing a q^{-4} slope at X = 0.80 as expected for smooth interfaces according to the Porod law. The most characteristic feature of the curve at X = 0.80 is however the presence of a weak peak at q_{peak} = 0.23 nm^{-1}, which suggests the existence of segregated nanoregions within the large aggregates with a characteristic packing distance $2\pi/q_{peak}$ of about 27 nm. The scattering profile of the charge equimolar sample (X = 0.50) suggests an intermediate situation. It includes features of both the X = 0.80 sample, reminiscent of microphase separation (the weak peak, a higher slope closer to the Porod-like behavior) and of the X = 0.33 sample, reminiscent of spherical aggregates (the oscillation with a minimum in the q range around 0.2 nm^{-1}).

Fits of the SAXS curves were also performed by modeling the scattering particles at 60 °C. The details of the fits are reported in chapter 3.2 of the Supplementary material. The coexistence of different structures was needed to reproduce the experimental curve. The contribution and the type of structures were observed to depend on the sample composition. For all the samples at X ≤ 0.50, the presence of free block copolymer chains and block copolymer micelles was needed. At X = 0 and 0.20, large spheres were used to account for the contribution of the clusters. At X = 0.20, a contribution of spherical mixed aggregates larger than the copolymer micelles (core radius of about 16 nm) was also needed in the data fitting. The size of these aggregates increased to about 20 nm at X = 0.33, where their scattering became dominant. This contribution was preserved at X = 0.50, where additional larger aggregates were observed with a diameter larger than 80 nm. At the highest BS content (X = 0.80) the fit was performed assuming a further growth of these large aggregates with a broad peak feature related to their internal structure. In addition, a contribution of NaDC micelles formed at this large surfactant fraction was also introduced.

Based on the DSC results, and supported by the results from the other techniques reported, we can now summarize the thermoresponsive behavior of the block copolymer-bile salt system. At low temperature, without any bile salt and well below the cloud point, the copolymer is present as single chains that coexist with loose multichain clusters according to previous studies on similar copolymers [42,43]. In this condition, the DLS autocorrelation function is dominated by the translational diffusion process of large clusters, which undergo a size shrinkage upon increasing the temperature (see inset of Fig. 3b). At the phase transition or cloud point, the aggregation process is accompanied by only a partial dehydration of the PNIPAM chains, which is reflected in a lower transition enthalpy as compared to the PNIPAM homopolymer (see Table 1). This result is in coherence with the DSC data reported for similar PNIPAM-*b*-PAMPTMA(+) block copolymers in water [42,87]. SAXS data demonstrate that free copolymer chains and a very little fraction of small micelles with a core of dehydrated PNIPAM blocks and a corona of PAMPTMA(+) blocks coexist with the clusters at 60 °C.

In the mixtures with the bile salt at room temperature, mixed complexes form through a preferential interaction between the cationic PAMPTMA(+) blocks and the DC^- anions [23]. The neutralization given by DC^- at X = 0.20 triggers an enhanced dehydration of the block copolymer at T_{cp} into denser aggregates, which scatter a higher intensity in the light scattering experiments (Fig. 2). This also explains the increase in cooperativity of the transition in comparison to the pure copolymer (see DSC scans in the inset of Fig. 5a and Table 1).

Above the transition, at 60 °C, the SAXS curve of the X = 0.20 sample shows that clusters, reasonably formed by partially DC^- anion-neutralized copolymer chains, and small copolymer micelles are kept as well as free chains. In addition, mixed aggregates with a core radius of about 16 nm, start to form. The corresponding DSC trace presenting a shoulder at higher temperature, supports the coexistence of different structures in this sample (Fig. 5a). Reasonably, the cooperative process occurring at lower temperature in the DSC trace of X = 0.20 results in the formation of the 16 nm mixed aggregates. For this aggregate, a core of densely packed PNIPAM chains and a corona of PAMPTMA(+) blocks largely neutralized by DC^- anions is proposed. The formation of looser and larger aggregates similar to the shrunken clusters of the pure block copolymer justifies the shoulder of the DSC peak.

As the content of NaDC is increased in the mixtures, larger fractions of copolymers are engaged in the interaction with BS molecules below the characteristic T_{onset}. This is reflected by that the low-temperature part of the DSC transition peak present at X = 0.20 increases in amplitude to finally dominate the thermogram at X ≥ 0.50 while T_{onset} decreases approaching a value close to about 32 °C (Fig. 5b). At the same time there is a significant increase in the cooperativity of the transition (see the corresponding ΔH_{tr} in Table 1). At temperatures above the phase transition, the SAXS data analysis suggests that further addition of bile salt determines the disappearance of the clusters and a slight growth of the mixed aggregates, whose radii become about 20 nm at X = 0.33 and 0.50. At X = 0.50, a further population of aggregates with radius of

about 40 nm is observed to contribute to the SAXS intensities, which are probably the prelude to the precipitation observed at higher X values. Interestingly the sizes of these aggregates are in agreement with those inferred from DLS measurements ($\langle D_H \rangle \approx 80$ nm) where they are expected to contribute the most.

It is interesting to note that the light scattering intensity is the highest at X = 0.20 and it decreases at higher X values (0.33 and 0.50) in parallel with the disappearance of the clusters (Fig. 2). This indicates that the clusters are the main responsible of the light scattering at X = 0.20. Since the scattered light intensity of the shrunken clusters in the pure block copolymer solution at 60 °C is very low (black symbols in Fig. 2), we envision that the added BS at X = 0.20 should essentially be included into the clusters. This supports the hypothesis that the small micelles, the spherical mixed aggregates and maybe the free copolymer chains inferred from the fit at X = 0.20 are all included in the cluster, which therefore might be described as a structure factor rather than a separate structure.

SAXS curves demonstrate that further addition of NaDC up to X = 0.80 promotes a co-assembly into copolymer-bile salt aggregates with a microphase-separated interior consisting of nanoregions of dehydrated PNIPAM and PAMTPMA(+)/DC$^-$. The microphase-separated nanoregions have an inter-distance of about 27 nm according to the peak position in the SAXS profile. A similar situation has been discussed in the study by Ferreira et al. [96], where domains consistent with immiscible poly(acrylamide) (PAAm) and poly(acrylate) (PAA$^-$)/cetyltrimethyl ammonium (CTA$^+$) were found in block copolymer complex salts formed using PAAm-*b*-PAA block copolymers and *n*-alkyltrimethylammonium cationic surfactants.

4. Conclusions

Development of nanotechnology has constantly increased the demand of smart nanocarrier systems for inclusion, transport and delivery of biomolecules or active drug substances. Systems with tunable responsiveness are particularly appealing, as they become versatile nanomaterials that can be easily adapted to application conditions. Biocompatibility is another important feature of the nanostructures as it makes them suitable for environmentally friendly and biomedical applications.

We have earlier demonstrated that thermoresponsive cationic block copolymer PNIPAM$_{120}$-*b*-PAMPTMA(+)$_{30}$ and a natural bile salt NaDC form intriguing nanostructures at room temperature [23]. In this study the effect of temperature on the association in the same system was investigated. We found that the loss of water-solubility of PNIPAM with increasing temperature induces pronounced aggregation at a transition temperature that can be modified by controlling the stoichiometry of the mixture. Without NaDC, the phase transition temperature of the copolymer solution is far above that of pure PNIPAM homopolymer solution. For the mixed solutions, however, the interaction between the copolymer and bile salt leads to a continuous decrease in transition temperature with increasing bile salt content, approaching 32 °C for samples with high bile salt fraction. The mixture composition also allows the control over the charge of the aggregates formed at higher temperatures. The co-assembled mixed complexes at low and ambient temperatures are almost neutral while at elevated temperatures, aggregates containing dehydrated PNIPAM form that become remarkably positive or negative depending on whether the cationic block copolymer or the anionic bile salt dominates the mixture composition in terms of charge fraction.

With these results, our study discloses a potential of cationic block copolymer-bile salt mixtures for the preparation of versatile smart material and incentivize an extended analysis to different type of block copolymers and natural steroidal surfactants. It also provides important information about the use of cationic PNIPAM-based block copolymers as bile salt sequestrants in the treatment of hypercholesterolemia and bile acid diarrhea. Indeed, the results presented here show that at body temperature, the low solubility of PNIPAM strongly affects the block copolymer-bile salt association and induces precipitation at large excess of bile salt, thus providing a premise of the behavior of the block copolymer when introduced in the gastrointestinal track as a sequestrant.

CRediT authorship contribution statement

Guanqun Du: Investigation, Formal analysis, Validation, Visualization, Writing - original draft, Writing - review & editing. **Alessandra Del Giudice:** Investigation, Formal analysis, Visualization, Writing - review & editing. **Viveka Alfredsson:** Writing - review & editing. **Anna M. Carnerup:** Resources. **Nicolae V. Pavel:** Investigation, Writing - review & editing. **Watson Loh:** Writing - review & editing. **Giancarlo Masci:** Resources. **Bo Nyström:** Writing - review & editing. **Luciano Galantini:** Conceptualization, Methodology, Resources, Supervision, Investigation, Writing - review & editing, Funding acquisition. **Karin Schillén:** Conceptualization, Methodology, Investigation, Resources, Supervision, Data curation, Writing - original draft, Writing - review & editing, Project administration, Funding acquisition.

Declaration of competing interest

The authors declare that they have no known competing financial interests or personal relationships that could have appeared to influence the work reported in this paper.

Acknowledgments

We thank Björn Lindman and Matija Tomšič for fruitful and stimulating discussions and Alessio di Giuseppe for performing part of the light scattering and electrophoretic mobility measurements. The SOLEIL synchrotron Facility, Saint-Aubin, France is acknowledged for providing beam-time and lab facilities (ID20160186) and we would like to thank Javier Pérez for the relevant assistance at the SWING beamline. K. Schillén kindly acknowledges the Sapienza Visiting Professor Programme 2018 for the visiting professorship grant. G. Du acknowledges the China Scholarship Council (CSC) for the PhD scholarship. This work was supported by The Swedish Research Council (VR) [grant number 621-2013-4339]; Magnus Bergvalls Stiftelse, Stockholm, Sweden [grant number 2017-02225]; and The Crafoord Foundation [grant number 20180549], Lund, Sweden.

Appendix A. Supplementary data

Supplementary data to this article can be found online at https://doi.org/10.1016/j.polymer.2020.122871.

References

[1] M.A.C. Stuart, W.T.S. Huck, J. Genzer, M. Müller, C. Ober, M. Stamm, G. B. Sukhorukov, I. Szleifer, V.V. Tsukruk, M. Urban, F. Winnik, S. Zauscher, I. Luzinov, S. Minko, Emerging applications of stimuli-responsive polymer materials, Nat. Mater. 9 (2010) 101–113, https://doi.org/10.1038/nmat2614.
[2] L. Chiappisi, I. Hoffmann, M. Gradzielski, Complexes of oppositely charged polyelectrolytes and surfactants - recent developments in the field of biologically derived polyelectrolytes, Soft Matter 9 (2013) 3896–3909, https://doi.org/10.1039/c3sm27698h.
[3] N. Khan, B. Brettmann, Intermolecular interactions in polyelectrolyte and surfactant complexes in solution, Polymers 11 (2019) 51, https://doi.org/10.3390/polym11010051.
[4] E. Guzmán, L. Fernández-Peña, F. Ortega, R.G. Rubio, Equilibrium and kinetically trapped aggregates in polyelectrolyte–oppositely charged surfactant mixtures, Curr. Opin. Colloid Interface Sci. 48 (2020) 91–108, https://doi.org/10.1016/j.cocis.2020.04.002.
[5] A.F. Hofmann, K.J. Mysels, Bile salts as biological surfactants, Colloids Surf., A 30 (1987) 145–173, https://doi.org/10.1016/0166-6622(87)80207-X.
[6] M.J. Monte, J.J.G. Marin, A. Antelo, J. Vazquez-Tato, Bile acids: chemistry, physiology, and pathophysiology, World J. Gastroenterol. 15 (2009) 804, https://doi.org/10.3748/wjg.15.804.

[7] M. Cárdenas, K. Schillén, V. Alfredsson, R.D. Duan, L. Nyberg, T. Arnebrant, Solubilization of sphingomyelin vesicles by addition of a bile salt, Chem. Phys. Lipids 151 (2008) 10–17, https://doi.org/10.1016/j.chemphyslip.2007.09.002.

[8] T. Lundåsen, C. Gälman, B. Angelin, M. Rudling, Circulating intestinal fibroblast growth factor 19 has a pronounced diurnal variation and modulates hepatic bile acid synthesis in man, J. Intern. Med. 260 (2006) 530–536, https://doi.org/10.1111/j.1365-2796.2006.01731.x.

[9] J.R.F. Walters, A.M. Tasleem, O.S. Omer, W.G. Brydon, T. Dew, C.W. le Roux, A new mechanism for bile acid diarrhea: defective feedback inhibition of bile acid biosynthesis, Clin. Gastroenterol. Hepatol. 7 (2009) 1189–1194, https://doi.org/10.1016/j.cgh.2009.04.024.

[10] I. Johnston, J. Nolan, S.S. Pattni, J.R.F. Walters, New insights into bile acid malabsorption, Curr. Gastroenterol. Rep. 13 (2011) 418–425, https://doi.org/10.1007/s11894-011-0219-3.

[11] J.R.F. Walters, Bile acid diarrhoea and FGF19: new views on diagnosis, pathogenesis and therapy, Nat. Rev. Gastroenterol. Hepatol. 11 (2014) 428–434, https://doi.org/10.1038/nrgastro.2014.32.

[12] P. Zarras, O. Vogl, Polycationic salts as bile acid sequestering agents, Prog. Polym. Sci. 24 (1999) 485–516, https://doi.org/10.1016/S0079-6700(99)00002-7.

[13] C.C. Huval, S.R. Holmes-Farley, W.H. Mandeville, R. Sacchiero, P.K. Dhal, Syntheses of hydrophobically modified cationic hydrogels by copolymerization of alkyl substituted diallylamine monomers and their use as bile acid sequestrants, Eur. Polym. J. 40 (2004) 693–701, https://doi.org/10.1016/j.eurpolymj.2003.11.012.

[14] J.R.F. Walters, S.S. Pattni, Managing bile acid diarrhoea, Therap. Adv. Gastroenterol. 3 (2010) 349–357, https://doi.org/10.1177/1756283X10377126.

[15] C. Wilcox, J. Turner, J. Green, Systematic review: the management of chronic diarrhoea due to bile acid malabsorption, Aliment. Pharmacol. Ther. 39 (2014) 923–939, https://doi.org/10.1111/apt.12684.

[16] W.H. Mandeville, D.I. Goldberg, The sequestration of bile acids, a non-absorbed method for cholesterol reduction. A review, Curr. Pharmaceut. Des. 3 (1997) 15–28.

[17] M. Camilleri, G.J. Gores, Therapeutic targeting of bile acids, Am. J. Physiol. Gastrointest. Liver Physiol. 309 (2015) G209–G215, https://doi.org/10.1152/ajpgi.00121.2015.

[18] M. Hansen, D.P. Sonne, F.K. Knop, Bile acid sequestrants: glucose-lowering mechanisms and efficacy in type 2 diabetes, Curr. Diabetes Rep. 14 (2014) 482, https://doi.org/10.1007/s11892-014-0482-4.

[19] P.V. Mendonça, A.C. Serra, C.L. Silva, S. Simões, J.F.J. Coelho, Polymeric bile acid sequestrants - synthesis using conventional methods and new approaches based on “controlled”/living radical polymerization, Prog. Polym. Sci. 38 (2013) 445–461, https://doi.org/10.1016/j.progpolymsci.2012.09.004.

[20] E. Heřmánková, A. Žák, L. Poláková, R. Hobzová, R. Hromádka, J. Širc, Polymeric bile acid sequestrants: review of design, in vitro binding activities, and hypocholesterolemic effects, Eur. J. Med. Chem. 144 (2018) 300–317, https://doi.org/10.1016/j.ejmech.2017.12.015.

[21] N.S. Cameron, A. Eisenberg, G.R. Brown, Amphiphilic block copolymers as bile acid sorbents: 1. Synthesis of polystyrene-*b*-poly(*N*,*N*,*N*-trimethylammoniumethylene acrylamide chloride), Biomacromolecules 3 (2002) 116–123, https://doi.org/10.1021/bm015595k.

[22] N.S. Cameron, A. Eisenberg, G.R. Brown, Amphiphilic block copolymers as bile acid sorbents: 2. Polystyrene-*b*-poly(*N*,*N*,*N*-trimethylammoniumethylene acrylamide chloride): self-assembly and application to serum cholesterol reduction, Biomacromolecules 3 (2002) 124–132, https://doi.org/10.1021/bm015596c.

[23] K. Schillén, L. Galantini, G. Du, A. Del Giudice, V. Alfredsson, A.M. Carnerup, N. V. Pavel, G. Masci, B. Nyström, Block copolymers as bile salt sequestrants: intriguing structures formed in a mixture of an oppositely charged amphiphilic block copolymer and bile salt, Phys. Chem. Chem. Phys. 21 (2019) 12518–12529, https://doi.org/10.1039/c9cp01744e.

[24] S. Bayati, L. Galantini, K.D. Knudsen, K. Schillén, Effects of bile salt sodium glycodeoxycholate on the self-assembly of PEO-PPO-PEO triblock copolymer P123 in aqueous solution, Langmuir 31 (2015) 13519–13527, https://doi.org/10.1021/acs.langmuir.5b03828.

[25] S. Bayati, L. Galantini, K.D. Knudsen, K. Schillén, Complexes of PEO-PPO-PEO triblock copolymer P123 and bile salt sodium glycodeoxycholate in aqueous solution: a small angle X-ray and neutron scattering investigation, Colloids Surfaces A Physicochem. Eng. Asp. 504 (2016) 426–436, https://doi.org/10.1016/j.colsurfa.2016.05.096.

[26] S. Bayati, C. Anderberg Haglund, N.V. Pavel, L. Galantini, K. Schillén, Interaction between bile salt sodium glycodeoxycholate and PEO-PPO-PEO triblock copolymers in aqueous solution, RSC Adv. 6 (2016) 69313–69325, https://doi.org/10.1039/c6ra12514j.

[27] V. Patel, D. Ray, A. Bahadur, J. Ma, V.K. Aswal, P. Bahadur, Pluronic®-bile salt mixed micelles, Colloids Surf., B 166 (2018) 119–126, https://doi.org/10.1016/j.colsurfb.2018.03.001.

[28] W. Brown, K. Schillén, M. Almgren, S. Hvidt, P. Bahadur, Micelle and gel formation in a poly(ethylene oxide)/poly(propylene oxide)/poly(ethylene oxide) triblock copolymer in water solution. Dynamic and static light scattering and oscillatory shear measurements, J. Phys. Chem. 95 (1991) 1850–1858, https://doi.org/10.1021/j100157a064.

[29] W. Brown, K. Schillén, S. Hvidt, Triblock copolymers in aqueous solution studied by static and dynamic light scattering and oscillatory shear measurements. Influence of relative block sizes, J. Phys. Chem. 96 (1992) 6038–6044, https://doi.org/10.1021/j100193a072.

[30] P. Alexandridis, J.F. Holzwarth, T.A. Hatton, Micellization of poly(ethylene oxide)-poly(propylene oxide)-poly(ethylene oxide) triblock copolymers in aqueous solutions: thermodynamics of copolymer association, Macromolecules 27 (1994) 2414–2425, https://doi.org/10.1021/ma00087a009.

[31] S. Manet, A. Lecchi, M. Impéror-Clerc, V. Zholobenko, D. Durand, C.L.P. Oliveira, J.S. Pedersen, I. Grillo, F. Meneau, C. Rochas, Structure of micelles of a nonionic block copolymer determined by SANS and SAXS, J. Phys. Chem. B 115 (2011) 11318–11329, https://doi.org/10.1021/jp200212g.

[32] A.V. Kabanov, E.V. Batrakova, V.Y. Alakhov, Pluronic® block copolymers as novel polymer therapeutics for drug and gene delivery, J. Contr. Release 82 (2002) 189–212, https://doi.org/10.1016/S0168-3659(02)00009-3.

[33] A.M. Bodratti, P. Alexandridis, Formulation of poloxamers for drug delivery, J. Funct. Biomater. 9 (2018) 11, https://doi.org/10.3390/jfb9010011.

[34] M.T. Calejo, A.M.S. Cardoso, A.-L. Kjøniksen, K. Zhu, C.M. Morais, S.A. Sande, A. L. Cardoso, M.C.P. De Lima, A. Jurado, B. Nyström, Temperature-responsive cationic block copolymers as nanocarriers for gene delivery, Int. J. Pharm. 448 (2013) 105–114, https://doi.org/10.1016/j.ijpharm.2013.03.028.

[35] C.M. Schilli, M. Zhang, E. Rizzardo, S.H. Thang, Y.K. Chong, K. Edwards, G. Karlsson, A.H.E. Müller, A new double-responsive block copolymer synthesized via RAFT polymerization: poly(*N*-isopropylacrylamide)-block-poly(acrylic acid), Macromolecules 37 (2004) 7861–7866, https://doi.org/10.1021/ma035838w.

[36] G. Masci, M. Diociaiuti, V. Crescenzi, ATRP synthesis and association properties of thermoresponsive anionic block copolymers, J. Polym. Sci. Part A Polym. Chem. 46 (2008) 4830–4842, https://doi.org/10.1002/pola.22816.

[37] A.-L. Kjøniksen, K. Zhu, R. Pamies, B. Nyström, Temperature-induced formation and contraction of micelle-like aggregates in aqueous solutions of thermoresponsive short-chain copolymers, J. Phys. Chem. B 112 (2008) 3294–3299, https://doi.org/10.1021/jp800404a.

[38] M.L. Patrizi, M. Diociaiuti, D. Capitani, G. Masci, Synthesis and association properties of thermoresponsive and permanently cationic charged block copolymers, Polymer 50 (2009) 467–474, https://doi.org/10.1016/j.polymer.2008.11.023.

[39] A.-L. Kjøniksen, K. Zhu, M.A. Behrens, J.S. Pedersen, B. Nyström, Effects of temperature and salt concentration on the structural and dynamical features in aqueous solutions of charged triblock copolymers, J. Phys. Chem. B 115 (2011) 2125–2139, https://doi.org/10.1021/jp1075884.

[40] M.A. Behrens, M. Lopez, A.-L. Kjøniksen, K. Zhu, B. Nyström, J.S. Pedersen, Structure and interactions of charged triblock copolymers studied by small-angle X-ray scattering: dependence on temperature and charge screening, Langmuir 28 (2012) 1105–1114, https://doi.org/10.1021/la202841q.

[41] M.A. Behrens, A.-L. Kjøniksen, K. Zhu, B. Nyström, J.S. Pedersen, Small-angle X-ray scattering study of charged triblock copolymers as a function of polymer concentration, temperature, and charge screening, Macromolecules 45 (2012) 246–255, https://doi.org/10.1021/ma2016216.

[42] G. Lazzara, G. Olofsson, V. Alfredsson, K. Zhu, B. Nyström, K. Schillén, Temperature-responsive inclusion complex of cationic PNIPAAM diblock copolymer and γ-cyclodextrin, Soft Matter 8 (2012) 5043–5054, https://doi.org/10.1039/c2sm07252a.

[43] S. Bayati, K. Zhu, L.T.T. Trinh, A.-L. Kjøniksen, B. Nyström, Effects of temperature and salt addition on the association behavior of charged amphiphilic diblock copolymers in aqueous solution, J. Phys. Chem. B 116 (2012) 11386–11395, https://doi.org/10.1021/jp306833x.

[44] E. Karjalainen, N. Chenna, P. Laurinmäki, S.J. Butcher, H. Tenhu, Diblock copolymers consisting of a polymerized ionic liquid and poly(*N*-isopropylacrylamide). Effects of PNIPAM block length and counter ion on self-assembling and thermal properties, Polym. Chem. 4 (2013) 1014–1024, https://doi.org/10.1039/c2py20815f.

[45] A. Papagiannopoulos, J. Zhao, G. Zhang, S. Pispas, A. Radulescu, Thermoresponsive transition of a PEO-*b*-PNIPAM copolymer: from hierarchical aggregates to well defined ellipsoidal vesicles, Polymer 54 (2013) 6373–6380, https://doi.org/10.1016/j.polymer.2013.09.016.

[46] T. Sato, K. Tanaka, A. Toyokura, R. Mori, R. Takahashi, K. Terao, S.I. Yusa, Self-association of a thermosensitive amphiphilic block copolymer poly(*N*-isopropylacrylamide)-*b*-poly(*N*-vinyl-2-pyrrolidone) in aqueous solution upon heating, Macromolecules 46 (2013) 226–235, https://doi.org/10.1021/ma3020992.

[47] R. Takahashi, X.P. Qiu, N. Xue, T. Sato, K. Terao, F.M. Winnik, Self-association of the thermosensitive block copolymer poly(2-isopropyl-2-oxazoline)-*b*-poly(*N*-isopropylacrylamide) in water-methanol mixtures, Macromolecules 47 (2014) 6900–6910, https://doi.org/10.1021/ma501538t.

[48] S.K. Filippov, A. Bogomolova, L. Kaberov, N. Velychkivska, L. Starovoytova, Z. Cernochova, S.E. Rogers, W.M. Lau, V.V. Khutoryanskiy, M.T. Cook, Internal nanoparticle structure of temperature-responsive self-assembled PNIPAM-*b*-PEG-*b*-PNIPAM triblock copolymers in aqueous solutions: NMR, SANS, and light scattering studies, Langmuir 32 (2016) 5314–5323, https://doi.org/10.1021/acs.langmuir.6b00284.

[49] N.S. Vishnevetskaya, V. Hildebrand, B.J. Niebuur, I. Grillo, S.K. Filippov, A. Laschewsky, P. Müller-Buschbaum, C.M. Papadakis, Aggregation behavior of doubly thermoresponsive polysulfobetaine-*b*-poly(*N*-isopropylacrylamide) diblock copolymers, Macromolecules 49 (2016) 6655–6668, https://doi.org/10.1021/acs.macromol.6b01186.

[50] M.T. Cook, S.K. Filippov, V.V. Khutoryanskiy, Synthesis and solution properties of a temperature-responsive PNIPAM–*b*-PDMS–*b*-PNIPAM triblock copolymer, Colloid Polym. Sci. 295 (2017) 1351–1358, https://doi.org/10.1007/s00396-017-4084-y.

[51] I.A. Van Hees, P.J.M. Swinkels, R.G. Fokkink, A.H. Velders, I.K. Voets, J. Van Der Gucht, M. Kamperman, Self-assembly of oppositely charged polyelectrolyte block copolymers containing short thermoresponsive blocks, Polym. Chem. 10 (2019) 3127–3134, https://doi.org/10.1039/c9py00250b.

[52] C. Kuang, S.I. Yusa, T. Sato, Micellization and phase separation in aqueous solutions of thermosensitive block copolymer poly(*N*-isopropylacrylamide)-*b*-poly (*N*-vinyl-2-pyrrolidone) upon heating, Macromolecules 52 (2019) 4812–4819, https://doi.org/10.1021/acs.macromol.9b00807.
[53] C. Wu, S. Zhou, Laser light scattering study of the phase transition of poly(*N*-isopropylacrylamide) in water. 1. Single chain, Macromolecules 28 (1995) 8381–8387, https://doi.org/10.1021/ma00128a056.
[54] L.T. Lee, B. Cabane, Effects of surfactants on thermally collapsed poly(*N*-isopropylacrylamide) macromolecules, Macromolecules 30 (1997) 6559–6566, https://doi.org/10.1021/ma9704469.
[55] Y. Okada, F. Tanaka, Cooperative hydration, chain collapse, and flat LCST behavior in aqueous poly(*N*-isopropylacrylamide) solutions, Macromolecules 38 (2005) 4465–4471, https://doi.org/10.1021/ma0502497.
[56] V.O. Aseyev, H. Tenhu, F.M. Winnik, Temperature dependence of the colloidal stability of neutral amphiphilic polymers in water, Adv. Polym. Sci. 196 (2006) 1–85, https://doi.org/10.1007/12_052.
[57] F. Tanaka, T. Koga, F.M. Winnik, Temperature-responsive polymers in mixed solvents: competitive hydrogen bonds cause cononsolvency, Phys. Rev. Lett. 101 (2008) 28302, https://doi.org/10.1103/PhysRevLett.101.028302.
[58] T. Kawaguchi, K. Kobayashi, M. Osa, T. Yoshizaki, Is a cloud-point curve in aqueous poly(*N*-isopropylacrylamide) solution binodal? J. Phys. Chem. B 113 (2009) 5440–5447, https://doi.org/10.1021/jp9005795.
[59] R. Pelton, Poly(*N*-isopropylacrylamide) (PNIPAM) is never hydrophobic, J. Colloid Interface Sci. 348 (2010) 673–674, https://doi.org/10.1016/j.jcis.2010.05.034.
[60] V. Aseyev, H. Tenhu, F.M. Winnik, Non-ionic thermoresponsive polymers in water, Adv. Polym. Sci. 242 (2011) 29–89, https://doi.org/10.1007/12_2010_57.
[61] M. Alaghemandi, E. Spohr, Molecular dynamics investigation of the thermo-responsive polymer poly(*N*-isopropylacrylamide), Macromol. Theory Simul. 21 (2012) 106–112, https://doi.org/10.1002/mats.201100071.
[62] D. Roy, W.L.A. Brooks, B.S. Sumerlin, New directions in thermoresponsive polymers, Chem. Soc. Rev. 42 (2013) 7214–7243, https://doi.org/10.1039/c3cs35499g.
[63] M. Heskins, J.E. Guillet, Solution properties of poly(*N*-isopropylacrylamide), J. Macromol. Sci. Part A - Chem. A2 (1968) 1441–1455, https://doi.org/10.1080/10601326808051910.
[64] A. Halperin, M. Kröger, F.M. Winnik, Poly(*N*-isopropylacrylamide) phase diagrams: fifty years of research, Angew. Chem. Int. Ed. 54 (2015) 15342–15367, https://doi.org/10.1002/anie.201506663.
[65] H.G. Schild, Poly(*N*-isopropylacrylamide): experiment, theory and application, Prog. Polym. Sci. 17 (1992) 163–249, https://doi.org/10.1016/0079-6700(92)90023-R.
[66] R. Pamies, K. Zhu, A.-L. Kjøniksen, B. Nyström, Thermal response of low molecular weight poly(*N*-isopropylacrylamide) polymers in aqueous solution, Polym. Bull. 62 (2009) 487–502, https://doi.org/10.1007/s00289-008-0029-4.
[67] M.C. Di Gregorio, M. Gubitosi, L. Travaglini, N.V. Pavel, A. Jover, F. Meijide, J. Vázquez Tato, S. Sennato, K. Schillén, F. Tranchini, S. De Santis, G. Masci, L. Galantini, Supramolecular assembly of a thermoresponsive steroidal surfactant with an oppositely charged thermoresponsive block copolymer, Phys. Chem. Chem. Phys. 19 (2017) 1504–1515, https://doi.org/10.1039/c6cp05665b.
[68] E. Moghimipour, A. Ameri, S. Handali, Absorption-enhancing effects of bile salts, Molecules 20 (2015) 14451–14473, https://doi.org/10.3390/molecules200814451.
[69] E. Tasca, A. Del Giudice, L. Galantini, K. Schillén, A.M. Giuliani, M. Giustini, A fluorescence study of the loading and time stability of doxorubicin in sodium cholate/PEO-PPO-PEO triblock copolymer mixed micelles, J. Colloid Interface Sci. 540 (2019) 593–601, https://doi.org/10.1016/j.jcis.2019.01.075.
[70] E. Tasca, P. Andreozzi, A. Del Giudice, L. Galantini, K. Schillén, A.M. Giuliani, M. de los Angeles Ramirez, S. Moya, M. Giustini, Poloxamer/sodium cholate co-formulation for micellar encapsulation of Doxorubicin with high efficiency for intracellular delivery: an in-vitro bioavailability study, J. Colloid Interface Sci. 579 (2020) 551–561, https://doi.org/10.1016/j.jcis.2020.06.096.
[71] L. Galantini, M.C. di Gregorio, M. Gubitosi, L. Travaglini, J.V. Tato, A. Jover, F. Meijide, V.H. Soto Tellini, N.V. Pavel, Bile salts and derivatives: rigid unconventional amphiphiles as dispersants, carriers and superstructure building blocks, Curr. Opin. Colloid Interface Sci. 20 (2015) 170–182, https://doi.org/10.1016/j.cocis.2015.08.004.
[72] M.C. Di Gregorio, L. Travaglini, A. Del Giudice, J. Cautela, N.V. Pavel, L. Galantini, Bile salts: natural surfactants and precursors of a broad family of complex amphiphiles, Langmuir 35 (2019) 6803–6821, https://doi.org/10.1021/acs.langmuir.8b02657.
[73] G. Masci, L. Giacomelli, V. Crescenzi, Atom transfer radical polymerization of *N*-isopropylacrylamide, Macromol. Rapid Commun. 25 (2004) 559–564, https://doi.org/10.1002/marc.200300140.
[74] J. Janiak, S. Bayati, L. Galantini, N.V. Pavel, K. Schillén, Nanoparticles with a bicontinuous cubic internal structure formed by cationic and non-ionic surfactants and an anionic polyelectrolyte, Langmuir 28 (2012) 16536–16546, https://doi.org/10.1021/la303938k.
[75] D.E. Koppel, Analysis of macromolecular polydispersity in intensity correlation spectroscopy: the method of cumulants, J. Chem. Phys. 57 (1972) 4814–4820, https://doi.org/10.1063/1.1678153.
[76] B.J. Frisken, Revisiting the method of cumulants for the analysis of dynamic light-scattering data, Appl. Optic. 40 (2001) 4087, https://doi.org/10.1364/ao.40.004087.
[77] G. David, J. Pérez, Combined sampler robot and high-performance liquid chromatography: a fully automated system for biological small-angle X-ray scattering experiments at the Synchrotron SOLEIL SWING beamline, J. Appl. Crystallogr. 42 (2009) 892–900, https://doi.org/10.1107/S0021889809029288.
[78] D. Orthaber, A. Bergmann, O. Glatter, SAXS experiments on absolute scale with Kratky systems using water as a secondary standard, J. Appl. Crystallogr. 33 (2000) 218–225, https://doi.org/10.1107/S0021889899015216.
[79] P. Tsolakis, G. Bokias, Temperature-sensitive water-soluble polyelectrolyte/surfactant complexes formed between dodecyltrimethylammonium bromide and a comb-type copolymer consisting of an anionic backbone and poly(*N*-isopropylacrylamide) side chains, Macromolecules 39 (2006) 393–398, https://doi.org/10.1021/ma051897t.
[80] M. Khimani, S.I. Yusa, V.K. Aswal, P. Bahadur, Aggregation behavior of double hydrophilic block copolymers in aqueous media, J. Mol. Liq. 276 (2019) 47–56, https://doi.org/10.1016/j.molliq.2018.11.135.
[81] G.A. Ferreira, L. Piculell, W. Loh, Addition of *n*-alcohols induces a variety of liquid-crystalline structures in surfactant-rich cores of dispersed block copolymer/surfactant nanoparticles, ACS Omega 1 (2016) 1104–1113, https://doi.org/10.1021/acsomega.6b00267.
[82] N.M. Carneiro, A.M. Percebom, W. Loh, Quest for thermoresponsive block copolymer nanoparticles with liquid-crystalline surfactant cores, ACS Omega 2 (2017) 5518–5528, https://doi.org/10.1021/acsomega.7b00905.
[83] H.G. Schild, D.A. Tirrell, Microcalorimetric detection of lower critical solution temperatures in aqueous polymer solutions, J. Phys. Chem. 94 (1990) 4352–4356, https://doi.org/10.1021/j100373a088.
[84] C. Boutris, E.G. Chatzi, C. Kiparissides, Characterization of the LCST behaviour of aqueous poly(*N*-isopropylacrylamide) solutions by thermal and cloud point techniques, Polymer 38 (1997) 2567–2570, https://doi.org/10.1016/S0032-3861(97)01024-0.
[85] Y. Ding, G. Zhang, Microcalorimetric investigation on association and dissolution of poly(*N*-isopropylacrylamide) chains in semidilute solutions, Macromolecules 39 (2006) 9654–9657, https://doi.org/10.1021/ma062269u.
[86] J.F. Lutz, Ö. Akdemir, A. Hoth, Point by point comparison of two thermosensitive polymers exhibiting a similar LCST: is the age of poly(NIPAM) over? J. Am. Chem. Soc. 128 (2006) 13046–13047, https://doi.org/10.1021/ja065324n.
[87] S. Bayati, K.E. Bergquist, K. Zhu, B. Nyström, J. Skov Pedersen, L. Galantini, K. Schillén, Mixed micelles of oppositely charged poly(*N*-isopropylacrylamide) diblock copolymers, J. Polym. Sci., Part B: Polym. Phys. 55 (2017) 1457–1470, https://doi.org/10.1002/polb.24403.
[88] H. Kouřilová, J. Spěváček, L. Hanyková, 1H NMR study of temperature-induced phase transitions in aqueous solutions of poly(*N*-isopropylmethacrylamide)/poly(*N*-vinylcaprolactam) mixtures, Polym. Bull. 70 (2013) 221–235, https://doi.org/10.1007/s00289-012-0831-x.
[89] W. Loh, L.A.C. Teixeira, L.T. Lee, Isothermal calorimetric investigation of the interaction of poly(*N*-isopropylacrylamide) and ionic surfactants, J. Phys. Chem. B 108 (2004) 3196–3201, https://doi.org/10.1021/jp037190v.
[90] H.G. Schild, D.A. Tirrell, Interaction of poly(*N*-isopropylacrylamide) with sodium *n*-alkyl sulfates in aqueous solution, Langmuir 7 (1991) 665–671, https://doi.org/10.1021/la00052a013.
[91] M. Osa, Y. Itoda, Y. Suzuki, T. Yumoto, A. Yoshida, A fluorescence probe study on the effects of surfactants on cloud points in aqueous poly(*N*-isopropylacrylamide) solutions, Polym. J. 47 (2015) 59–65, https://doi.org/10.1038/pj.2014.93.
[92] L. Pérez-Fuentes, D. Bastos-González, J. Faraudo, C. Drummond, Effect of organic and inorganic ions on the lower critical solution transition and aggregation of PNIPAM, Soft Matter 14 (2018) 7818–7828, https://doi.org/10.1039/c8sm01679h.
[93] Y. Xia, N.A.D. Burke, H.D.H. Stöver, End group effect on the thermal response of narrow-disperse poly(*N*-isopropylacrylamide) prepared by atom transfer radical polymerization, Macromolecules 39 (2006) 2275–2283, https://doi.org/10.1021/ma0519617.
[94] E.C. Cho, J. Lee, K. Cho, Role of bound water and hydrophobic interaction in phase transition of poly(*N*-isopropylacrylamide) aqueous solution, Macromolecules 36 (2003) 9929–9934, https://doi.org/10.1021/ma034851d.
[95] M.J. Tiera, G.R. dos Santos, V.A. Tiera, N.A.B. Vieira, E. Frolini, R.C. da Silva, W. Loh, Aqueous solution behavior of thermosensitive (*N*-isopropylacrylamide-acrylic acid-ethyl methacrylate) terpolymers, Colloid Polym. Sci. 283 (2005) 662–670, https://doi.org/10.1007/s00396-004-1198-9.
[96] G.A. Ferreira, L. Piculell, W. Loh, Hydration-dependent hierarchical structures in block copolymer-surfactant complex salts, Macromolecules 51 (2018) 9915–9924, https://doi.org/10.1021/acs.macromol.8b02053.